Article

Not peer-reviewed version

Chromaticity of Gromwell, Cape Jasmine Dyeing, and Effects of Zinc Oxide/Polyphenol Treatment with Copper Mordanting for UV Protection

Hye Jin Kim *

Posted Date: 15 May 2024

doi: 10.20944/preprints202405.1015.v1

Keywords: dye; xanthophyll; carotenoid; zinc oxide (ZnO); phenol; mordant; copper; K/S

doi:10.20944/preprints202405.1015.v1

Article

Chromaticity of Gromwell, Cape Jasmine Dyeing, and Effects of Zinc Oxide/Polyphenol Treatment with Copper Mordanting for UV Protection

Hye Jin Kim [1,2,3*]

[1] Graduate School of Design, Ewha Womans University, 03760, Korea
[2] Department of Fashion Industry, Ewha Womans University, 03760
[3] NewM Distance Lifelong Education Center, 07299, Korea
* Correspondence: vodratti@gmail.com; Tel.: +82 (0)10-4408-9361

Abstract: To protect skin from harmful ultraviolet (UV), zinc oxide (ZnO) with tannin from gallnuts was treated on cotton and polyester fabrics in this study. Before the treatments, the fabrics were dyed with shikonin and xanthophyll from Gromwell and Cape Jasmine. First, this study found that xanthophyll was more effective at preventing light fade or discoloration than shikonin. Despite the highest K/S, the untreated cotton in violet faded the most intensely when exposed to UV. The color variation of untreated polyester was narrow, with little change in L, a*, and K/S. Due to the non-photochemical xanthophyll, the yellow-dyed samples treated with ZnO/polyphenol did not vary yellowness (b*: 28.838) significantly, while the violet fabrics displayed a significant decrease in K/S and an increase in b*. The combination of ZnO and polyphenol treatment improved UV absorption at 350 to 250 nm. Cu-mordanting after ZnO/polyphenols treatment caused the violet cotton to turn reddish from blueish (negative to positive b*), with a hue change of 316° to 59° and the highest ΔE (25.90±4.34) after UV exposure. In this study, the combination of ZnO/polyphenol with Cu-mordants contributed the xanthophyll-dyed polyester to achieve a minimum ΔE and keep chroma and hue after UV exposure.

Keywords: dye; xanthophyll; carotenoid; zinc oxide (ZnO); phenol; mordant; copper; K/S;

1. Introduction

Ultraviolet (UV) radiation exposure can cause skin aging and inflammation due to the damage to collagen, hyaluronic acid, and protein [1–4]. Some functional fabrics can protect the skin exposed to UV rays by absorbing, transmitting, and reflecting UV light. For the functionalization of UV protective fabrics, the insertion of colorants onto the fabric surface, viz., dyeing, can manipulate light transmission, thereby resulting in photo stabilizing effects when the dyed fabrics shield UV illumination from 290 to 400 nm wavelength. On the other hand, UV-absorbing or shielding materials such as titanium dioxide and zinc oxide need to be incorporated.

Several researchers have studied how to adsorb zinc oxide (ZnO) nanoparticles onto cotton fabrics. The potential characteristics of ZnO are appropriate for UV protective materials, such as easy processibility, cost accessibility, biocompatibility, great electron mobility with high excitation binding energy, air-thermal stability, intensive photocatalytic ability, corrosion stability, and solar-UV absorption ability [5–9]. Belay et al. could increase the UV protection factor (UPF) of cotton fabrics coated with ZnO nanoparticles via in-situ deposition, compared with the precipitation method [10]. According to Rise et al., the UV absorption wavelength of ZnO stands out at 368 nm, equivalent to the band gap at 3.37 eV [11]. For optimal UV protection, it is adequate for sun-blocking materials to cover the wide range of UV absorption, including UVA and UVB.

With the aforementioned excellence of ZnO, another UV protective material is also required to strengthen the absorption range of ZnO. Several researchers have recently discovered organic UV absorbers from plant extracts for marine organisms, algae [12–17]. Regardless of its non-toxicity, mycosporine and its derivatives are expensive for practical use, compared with phenolic compounds from natural plant extracts. Polyphenols, one of the typical phytochemicals, can provide skin photoprotection [2,4]. Tannins of the polyphenols are mostly contained in berries, pomegranates, and green tea leaves [4,12]. The tannins from phenolic compounds can also be used as antioxidants. He et al. used polyphenols to scavenge free radicals from the hydroxyl groups of polyphenols, thereby inhibiting the generation of radicals and polymerization of photosensitive ink via the formation of quinones [18]. However, it is known for polyphenolic compounds to discolor and decolorize its applied fibers and textiles, resulting in poor color fastness to light. Overall, the possibility of discoloration by the polyphenols is controversial; hence, other factors in fadedness should also be considered, such as photodegradation in the manufacturing, storage, and usage processes.

As mentioned above, photodegradation can be classified into both internal material attributes and external environmental factors. Groeneveld et al. sorted the external factors as listed below: light irradiation, oxygen, temperature, and the internal factors: the inherent characteristics of colorants, photocatalysts, and textile substrates [19]. However, there are different photo mechanisms that excite different chromophores between visible and UV regions. According to Rader and Schmidtke [20], the concentration of oxygen can be another external factor since the rate of photodegradation can decrease in anaerobic environments because the oxidation causes decolorization by decomposing chromophores. The hydrogen ion exponent (pH) of dyeing solution, one of the internal factors, is a paramount cause of color change through photocatalyst oxidation. Not only the pH dye solution, but the type of textile substrate is also of vital importance. Nylon, wool, silk, and leather can easily be discolored or yellowed due to the chain scission of amino groups after being exposed to UV, nitrogen dioxide, ozone, moisture, and heat. Despite the weakness of proteinaceous fibers to photodegradation, acid dyeing enables wool to prevent discoloration or decolorization by neutralizing negative charges and forming cystine bonds on the woolen surface.

To minimize the decolorization affected by the factors mentioned above, it is necessary to understand photochemical mechanisms, which are dependent on the photon absorption of colorants or dye molecules. According to Michelin and Hoffmann, three photochemical mechanisms can be explained through direct or indirect photochemical reactions by photosensitizers, photocatalysts, and hydrogen, as follows: photoisomerization, photooxidation, and photoreduction [21]. Photoisomerization arises from the structural transformation of photocatalytic chromophores, for instance, chlorophylls glowing with autumn color into red, yellow, or brown. According to Abiola et al. (2020), trans-isomers of chromophores in natural dyes can be converted to *cis*-isomers when absorbing light irradiation of a short wavelength, resulting in discoloration of the dyed textiles [22]. Naphthoquinone, one of the quinonoid compounds, comprises many isomers, such as alkannin, lawsone, juglone, lapachol, plumbargin, and shikonin [23,24]. La and Giusti investigated the photochromism of delphinidins in anthocyanin dyes between *trans*- and cis-acylated isomers that were induced by visible UV light reversibly [25]. Carotenoids, one of the photoprotective dyes, are generated by the *cis-trans* isomerization of polar lutein and zeaxanthin, whereas the carotenoids turn into xanthophylls or *β*-cryptoxanthins due to the oxidation of the 3-hydroxy-*β*-end group of the xanthophyll [26]. The chromatic structures of chromophore groups can also be transformed by benzoyl peroxide, which causes the discoloration of their applied textiles. According to Rafiq et al., photooxidation occurs when photocatalytic dyes produce holes and electrons in excited states where photon absorption is higher than each bandgap energy of the photocatalytic dyes [27]. The chromophoric group photooxidates polyolefins by the generation of reactive oxygen species and hydrogen peroxide, then breaks down into hydroxyl and alkoxy radicals under Norrish and cage reactions, and finally terminates recombination in stabilized states [28]. On the other hand, photoreduction occurs when excited electrons, such as ketones, react with hydrogen from other molecular materials. The difference between photooxidation and photoreduction is the area of decolorization; for example, the only faded area of photo reduced fabrics is where they were exposed to light, whereas the area covered with wrinkles on other screens did not fade. In conclusion, discoloration can be prevented by dyeing fabrics with photo-protective colorants with

doi:10.20944/preprints202405.1015.v1

monochromaticity, by coordinating with metallic compounds, and by treating antioxidants and UV absorbers or blockers.

To avoid photodegradation, metal-polyphenolic chelating compounds can benefit from both metal cations donating electrons, hydrogen, and tannin against photooxidation. Catechol or gallol groups in the polyphenols play a role as ligands to chelate with metals, metal oxides, or carbon nanomaterials [13,14]. Feng et al. state that catechol's exceptional capacity to adsorb, attach, and bind to a variety of substrates, from hydrophilic to hydrophobic or from organic to inorganic surfaces, allows it to coordinate with metals such as Fe, Cu, Zn, and Al [14]. Wang et al. demonstrated that electroless deposition of ZnO and cotton surface modification could maintain high UPF mechanical properties even after 50 launderings with palladium as a catalyst and tannic acid as a linking agent [29]. The improvement in UV protection could be attributed to the fact that a large amount of ZnO and polyphenols from plant extracts were adsorbed onto inherently hollow cotton fibers, leading to UV absorption. The metal-polyphenolic coordination materials can result in synergistic effects on antioxidants and antiaging against the broad ranges of UV light, with tannins acting as organic UV absorbers and ZnO acting as inorganic UV blockers [3].

The purpose of this work was to functionalize UV-protective textiles using metallic mordanting, UV absorptive treatment, and natural coloring. Regarding the violet and yellow dyeing of cotton and polyester, two chromophores of naphthoquinone and β-carotenoid were extracted from plant roots and seeds, and FTIR investigations were then performed to identify the functional groups and dye constituents. To improve UV light absorption, zinc oxide and polyphenols were treated on the dyed fabrics. The reflectance analyses were demonstrated to prove the effectiveness of ZnO/polyphenol treatment by comparing the color differences (ΔE) between untreated and treated fabrics after UV exposure. Additionally, the color variation of four different metallic mordant types—particularly Cu-post mordanting—was examined using colorimetric metrics on the dyed materials, such as hue angle, chroma, a*, b*, and color depth (K/S).

2. Materials and Methods

2.1. Materials

In this study, violet and yellow in complementary colors were chosen to find the effects of mordanting, UV protective treatment, and exposure to UVC rays on the chromatic variation of dyed fabrics. As natural dyes, this work selected Gromwell roots (GWR) or Lithospermum erythrorhizon pellets (originated from China) and Cape jasmine seeds (CJS) or Gardenia jasminoides (originated from Korea). Both dyes were purchased at the Boncho Myeong-ga Industry-Daejeon University Cooperation Foundation. The extraction of GWR-Violet and CJS-Yellow dyes was conducted using anhydrous ethanol (purity 99%, Shicorp., Korea) and tertiary purified water (Joylife Corp., Korea), respectively. To facilitate the extraction of GWR-Violet dyes, 99% acetic acid (Samyang Ltd., Korea) was diluted. Zinc oxide (ZnO) and tannin as polyphenolic compounds, which derived from gallnut (Quercus infectoria) were selected to increase UV absorption in this research. The zinc oxide powder was obtained from Gooworl Corp., and the gallnut powder from Yongcheon Herb Medicine Farming Association Co., Ltd. (originated from China). The ZnO particles was dispersed in tertiary purified water and dimethyl sulfoxide (DMSO) (purity 99.8%, KisanBio, Korea).

To investigate the influence of post-mordanting on color variation, four mordants were used: aluminum potassium sulfate ($KAl(SO_4)_2$), copper acetate ($Cu(OAc)_2$), tin chloride ($SnCl_2$), and iron sulfate ($FeSO_4$). The aluminum potassium sulfate and iron sulfate were supplied from Sinsegi Science Corp. (Korea). Common copper plates were dissolved in diluted acetic acid (5 M) to make a copper acetate solution. A tin chloride solution was prepared by dissolving tin powder (96.5% Sn, 500 mesh) in 36.5% hydrochloric acid (Junsei Chemical Ltd., Japen). The tin powder was obtained from Juju Industry (Korea), whose size ranged from 25 μm to 80 μm.

2.2. Extraction of Natural Dyes and Preparation of Mordants

The first step was to extract the violet dyes from Gromwell roots (GWR), as shown in Figure 1 (a). 60 g of GWR pellets were mixed with 500 mL of ethanol. After diluting 50 mL of 5M acetic acid with tertiary filtered water, it was added to the GWR/ethanol solution. The solution was kept at room temperature for 72 hours with the container lid closed to prevent ethanol from evaporating. For the extraction of yellow dyes, 50 g of dried Cape Jasmine seeds (CJS), as seen in Figure 1(b), were soaked in 500 mL of water at 40 °C for 24 hours. After 24 hours, the first CJS-Yellow extract was filtered through a piece of muslin cloth into an Erlenmeyer flask, then left with its neck wrapped in aluminum foil. The residue seeds were extracted in another 500 mL of water in the second round, followed by the same procedure as above. After another 24 hours, the second CJS extract was added to the first dye solution for homogenization.

As shown in Figure 1(c-d), the second step was to prepare the photo-absorbers, zinc oxide powder, and crushed gallnut for UV protective treatment. The ZnO (6% o.w.f.) was dispersed in a 500 mL mixture of 350 mL of ethanol and 150 mL of purified water for the first treatment. For the second treatment, another 12% o.w.f. of ZnO powder was in 50 mL of DMSO. Both ZnO dispersed solutions were magnetically stirred for 60 mins, followed by ultrasonication for five mins. To extract pyrogallol acid from polyphenolic tannin, 25 g of gallnut was ground in a mortar with a pestle, and the residual dust was removed. 125 mL of purified water was poured into the ground gallnut, then boiled for one hour. After extracting the boiled solution, another 125 mL of water was added to the filtered gallnut, which was then boiled for another hour. Finally, all of the extracts were gathered into one container.

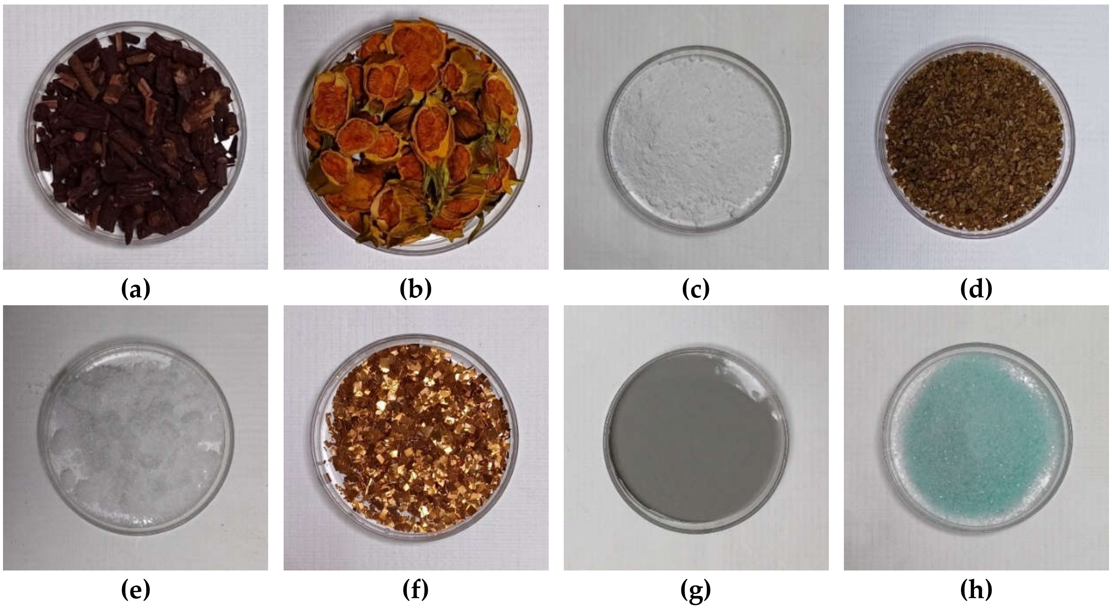

Figure 1. Photographs of **(a)** Gromwell root dyes, **(b)** Cape Jasmine seed dyes, **(c)** zinc oxide (ZnO), **(d)** gallnut, (e) aluminum potassium sulfate powder, **(f)** copper pieces for copper acetate solution, **(g)** tin powder for tin chloride solution, and **(h)** iron sulfate powder.

The next step was to dissolve metallic salts and thin metal pellets in each solvent for pre- and post-mordanting. The aluminum potassium sulfate (8% o.w.f.) and iron sulfate (2% o.w.f.) powders in Figure 1(e, h) were respectively stirred in distilled water of each 1 L for 60 mins and kept at room temperature to stabilize for another 60 mins. The copper plates were sliced into pieces ranging in size from 3 mm to 5 mm (Figure 1(f)). Then, 10 g of copper pellets were dissolved in a solution of 25 mL of purified water and 25 g of 5 M acetic acid. To accelerate the dissolving reaction, 9.7 M hydroperoxide was carefully added dropwise to the copper acetate solution and left at room temperature for 48 hours. The copper acetate solution turned blue, and the residual Cu pieces were filtered from the blue solution. For the preparation of tin chloride mordants, 2.457 g of tin power (500 mesh) was dissolved in 10 mL of 37% HCl in a three-neck reaction flask with rubber septa sealing and a magnet stirred at 75 °C. After 2 hours, 2 mL of purified water was added to the solution, then left on the hot plate without stirring for 12 hours. Finally, the tin chloride solution was cooled to room temperature for another 12 hours.

2.3. Natural Dyeing and Mordanting

In this study, two sets of cotton and polyester fabrics were dyed. Polyester nanofilament and organic cotton yarns were supplied by Kolon Fashion Material Ltd. and Hanjoong Union Ltd., respectively. Combed cotton for warp yarns was provided from Dong-A TOL Ltd., where weaving sampling was processed in this work.

As listed in Table 1, the first set for violet-dyeing were two types of twill-woven fabrics, made of (a) 100% cotton combed yarn (84.7 Nm) for both warp and weft and (b) the same cotton yarn for warp/polyester nanofilaments (8.33 tex) for weft. The second set for yellow-dyeing also included two types of satin-woven fabrics, comprising (c) 100% organic cotton (101.6 Nm) for weft with 100% cotton combed yarn (84.7 Nm) for warp and (d) the same cotton warp with polyester (8.33 tex). Each density (warp/weft) was as follows: (a) 172.5/110.4, (b) 104.0/104.0, (c) 145.7/122.8, and (d) 145.7/122.4 (unit: thds/inch). All fabrics were cut to 10 cm by 10 cm in size. Prior to dying, the cut fabrics were refined in tertiary purified water. After that, those were squeezed and dried at room temperature. For pre-mordanting, the fabrics were immersed in a $KAl(SO_4)_2$ solution for 20 minutes.

For dyeing in violet, first of all, 2 L of preheated water at 40 °C was poured into 100 mL of the Gromwell root extract. After being pre-mordanted, 15 g of wet twill fabrics were soaked in the extract. To prevent dye aggregation and bubble formation, the fabrics were turned over front and back and kept without floating. After 40 minutes, the violet-dyed fabrics were taken out of the extract, soaked in clean water for 10 minutes, and rinsed in flowing water. Finally, those were squeezed, dried in an oven at 35 °C, and ironed for wrinkle removal. This process is one cycle of violet dyeing. Before the second cycle, the dried fabrics were Al-mordanted repeatedly to strengthen color depth. As for yellow-dyeing, 27 g of wet satin fabrics were prepared as above. The fabrics were immersed in the Cape Jasmine extract in a bath ratio of 1:20 at 70 °C for 30 minutes. The other processes underwent the same process as violet dyeing.

The first UV protective treatment began between the third and fourth dyeing cycles. First, the dyed fabrics were immersed in the dispersion of ZnO in ethanol or water for 30 minutes, rinsed, squeezed, dried, and ironed, as aforementioned. For the second UV treatment, the four-time-dyed fabrics were soaked in the dispersion of ZnO in DMSO for 20 minutes, and the other procedure was identical to the previous one. As for the polyphenol treatment, half pieces of the ZnO-treated fabrics were put in the gallnut extract at 40 °C, then heated to 70 °C for 30 minutes. The ZnO and phenol were treated twice, respectively.

Post-mordanting started after the fifth dyeing cycle, except Al- pre-mordanting. First, 50 mL of copper acetate was poured into 1 L of purified water, and one fourth of the of the dyed fabrics were sunk into the diluted solution for 10 minutes. The Cu-mordanted fabrics were squeezed, soaked, rinsed in water, dried, and ironed. Then, Cu-post-mordanting was repeated for another 10 minutes. As for Sn-post-mordanting, 25 mL of tin chloride was diluted in 500 mL of distilled water. The other steps were the same as those of Cu-mordanting. The procedure for Fe-mordanting with iron sulfate powder was the same as above.

2.4. Exposure to UV-C and D65 Lamps

To evaluate the fadedness of dyed fabrics by UV or artificial lamps, a new design of UV testing apparatus was invented under the modification of ISO 105-B02:2014 Textiles in this research. In Figure 2, the apparatus consisted of illuminating sources, a rotating cylinder holding samples, a motor and its controller, and a chamber to block UV-C light. Figure 2(a) shows the open tetradecagonal cylinder of 17 cm in diameter with 14 pieces (w: 7 cm x h: 15 cm) to hold testing fabrics. The samples were cut at 2 cm x 5 cm. A couple of sample pieces were held inside with clips and tapes, as shown in Figure 2(b). A Xenon lamp was replaced with a 6500K LED lamp (60 Hz, 40W, Yuzhong Gaohong Ltd., China) and two UV-C lamps (8W, Osram, Italy, Phillips, Poland). The UV lamps were stuck with their backs to each other and hung on the chamber ceiling. The brushless DC motor (K8XH50N2, GGM, Korea) was rotating at a rate of 10.5 rpm during the testing (Figure 2(c)). The motor was connected to the PLC controller and touch screen, as seen in Figure 2(d). The testing samples were exposed to UV lamps twice per 10 hours and the D65 light for 20 hours. Total exposure time was 40 hours under the data-logged chamber condition at 30.3 °C and 27.8% RH average.

(a) **(b)** **(c)** **(d)**

Figure 2. Photographs of UV light exposure apparatus: **(a)** a tetradecagonal holder; **(b)** a rotating apparatus with a 6500K lamp; **(c)** a rotating DC motor with UV-C lamps; and **(d)** a PLC controller with a touch screen in the chamber.

2.5. Characterization and Chromatic Analyses

To investigate the components and functional groups of the natural dyes, attenuated Fourier transform infrared (ATR-FTIR) spectrometry (Invenio-R, Bruker, USA) was used. The FTIR measurement ranged from 400 cm^{-1} to 4000 cm^{-1}, at a resolution of 4.0. The spectral analyses were conducted using KnowItAll Informatic System 2024 (Wiley Science Solutions) and the OPUS (Bruker Optik GmbH) program.

To confirm the ZnO crystalline structure and the size of ZnO particles, the D/Max-2200/VPC (Rigaku, Japan) X-ray diffractometer (XRD) was employed. The measurement parameters of X-ray diffraction were set at 40 kV/30 mA with a scanning range of 2θ from 25° to 85°. The XRD peaks were analyzed with reference cards from the Joint Committee on Powder Diffraction Standards (JCPDS) database, and the ZnO size was estimated through the Debey-Scherrer equation using Origin Pro 2024 software (OriginLab, USA). The average ZnO particle size was calculated in the Debey-Scherrer equation [30]. The crystallite size (D_{hkl}) was estimated from Eq. (1):

$$D_{hkl} = \frac{\kappa\lambda}{\beta\cos\theta} \tag{1}$$

where κ, λ, β, θ are Scherrer' constant (normally considered as 0.9), wavelength of the x-ray beam (copper used in this study, λ 1.54184 Å), the full width at half maximum (FWHM) of the peak, and Bragg's angle, respectively.

To find the effects of various mordants and UV exposure on the color and UV absorbance of the dyed fabrics, the UV-3600i Plus (Shimadzu, Japan) was utilized to measure UV-vis-NIR spectra with its deuterium lamp and integrating sphere attachment. The reflectance in the UV-vis spectrum was measured at an interval of 2 nm, and the light source was automatically switched at 310 nm. The reflectance (R) was converted into color strength (K/S value) at 600 nm (λ_{max} GWR-V) and at 450 nm (λ_{max} CHS-Y) through Kubelka-Munk equation Eq. (2), as follows:

$$\frac{K}{S} = \frac{(1-R)^2}{2R} \tag{2}$$

From the UV-vis spectra, the chromaticity and color difference coordination were obtained under a standard observer at 10° via the OriginPro 2024 program. The reflectance spectrum was converted to colorimetric parameters L, a*, b* in CIELAB with color space (u′, v′) coordinates. The total color difference (ΔE) between a testing sample and a reference sample was summarized by Eq. (3) as follows:

$$\triangle \mathrm{E} = \sqrt{(\Delta \mathrm{L})^2 + (\Delta \mathrm{a})^2 + (\Delta \mathrm{b})^2} \tag{3}$$

where L, a*, b* values indicate the color differences in lightness (L), the amount of red/magenta (+) from green (-), and the amount of yellow (+) from blue (-) between reference and test samples. The values of chroma (C), and hue angle (H) were estimated by the following Eq.(4-5):

$$\mathrm{C} = \sqrt{a^{*2} + b^{*2}} \tag{4}$$

$$H = tan^{-1}\left(\frac{b^*}{a^*}\right), \qquad H_1 = \begin{cases} H & if\ H \geq 0 \\ H = 360^\circ & therwise \end{cases} \tag{5}$$

Based on the colorimetric parameters above, this study adopted the CIEDE 2000 and CMC formulae defined by the Color Measurement Committee of the Society of Dyers and Colorists for the optimum values of color difference. The weighing factors were set as follows: kL = 1.5, kC = 1.9, and CMC = 2:1 [31,32]. The values were converted through the ColoCalculator programs, which are provided by Lindbloom and Osram Inc. (MA, USA).

3. Results

3.1. ATR FTIR Analyses of Natural Dyes and XRD Analyses of Zinc Oxide

Using ATR-FTIR spectra, structural investigations were carried out to investigate the auxochromic and chromophoric groups of two dyes derived from natural plants. The yellow to orange color hue of Cape Jasmine seeds is derived from long conjugated double bonds of carotenoids that are categorized into carotenes and xanthophylls, with carbon, hydrogen in common, and oxygen existing in the only xanthophylls [33]. As a medicinal herb due to its antioxidants, antiinflammation, and detoxification, shikonin ($C_{16}H_{16}O_5$), one of the naphthoquinone compounds, is imparted its violet and purple hues by its naphthalene group (absorption peak at approximately 490, 520, and 560 nm) [34–36].

Figure 3 (a) identifies the IR spectroscopic results of two natural dyes. The prominent characteristic of both dyes was the broad peak of O-H stretching vibrations at 3298 cm^{-1} (GWR-Violet-dyes) and 3329 cm^{-1} (CJS-Yellow-dyes). [37,38]. In addition, carboxyl groups (C=O stretching) (1750 cm^{-1} to 1710 cm^{-1}) were found in each dye spectrum [34,39]. The presence of oxygen proved that the quinonoid component of CJS-Yellow dye was not β-carotene, where oxygen is absent, but xanthophyll [39]. Medium peaks of C-O functional groups can be seen at 1045 cm^{-1} in the yellow dyes and at 1022 cm^{-1} in the violet dyes. In common, each symmetric C-H stretching band from alkanes was also observed at 2924 cm^{-1} (GWR-Violet-dyes) and 2921.88 cm^{-1} (CJS-Yellow-dyes), respectively [34,37]. The C-H bending vibrations of GWR-Violet and CJS-Yellow dyes absorb at low wavenumbers of 779 to 739 cm^{-1} and 895 cm^{-1}.

Besides, both dyes were also characterized by an inherent peak. In the GWR-violet dyes, aromatic rings (C=C vibration) were also in naphthoquinone bands at 1562 cm^{-1} [40]. The CJS-Yellow dyes revealed a weak peak at 3009 cm^{-1}, which can be attributed to alkenyl C-H stretching bands. However, it was found that the violet dye and the yellow dye are respectively consistent with shikonin components from naphthoquinone and xanthophyll from β-carotenoid, based on the results of FTIR spectra.

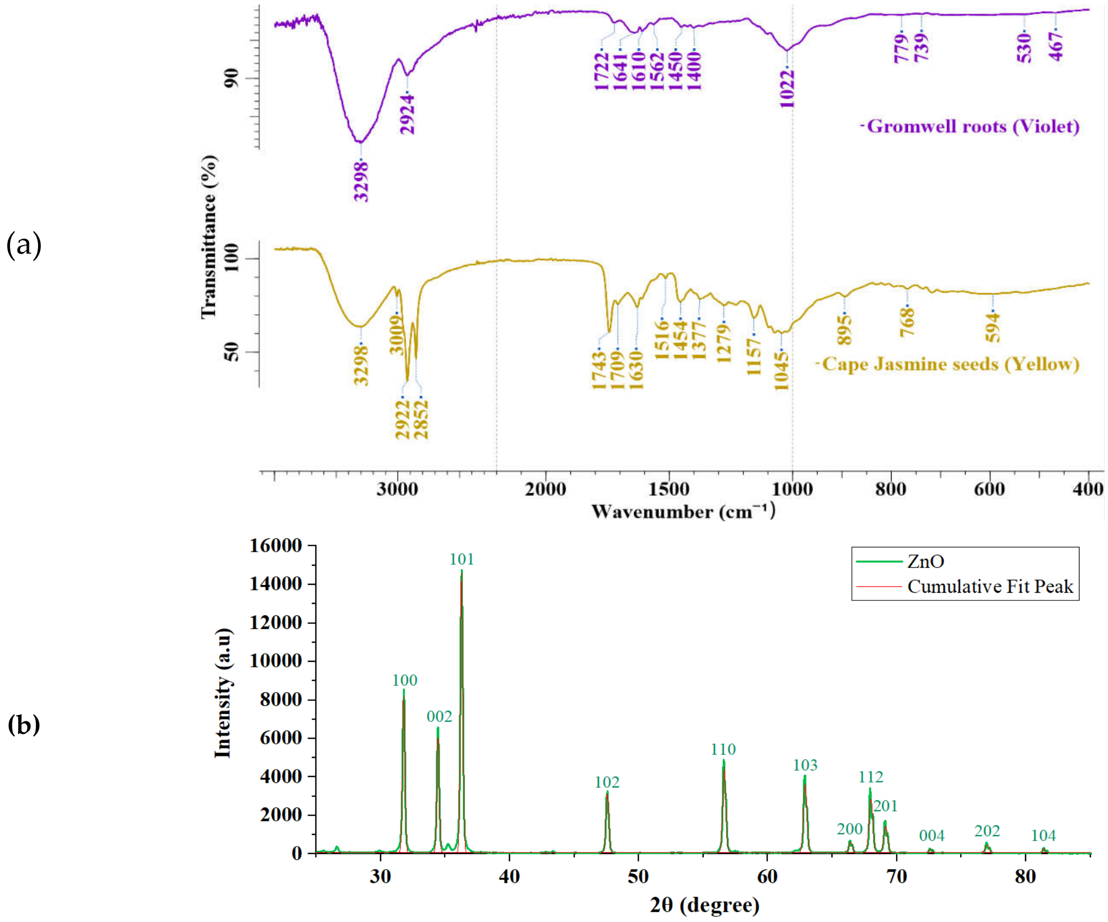

Figure 3. (a) Attenuated FTIR spectra of Gromwell roots-violet dyes, Cape Jasmine seeds-yellow dyes, and **(b)** XRD peaks of ZnO nanoparticles.

Twelve XRD peaks in Figure 3(b) verified ZnO wurtzite crystalline structure, which is in conformity with the JCPDS database reference (code: 01-079-2205). The structural patterns presented their hexagonal structure from the measured peaks (planes) at 31.76°(100), 31.76°(002), 34.42°(101), 36.26°(102), 47.54°(110), 56.60°(103), 66.36°(200), 67.96°(112), 69.08°(201), 72.58°(004), 76.96°(202), and 81.38°(104). The highest peak (17163.30 a.u.) was at 36.26° (101) plane with an atomic spacing of 37.494 nm. With Scherrer parameters, the ZnO crystallite size was estimated from the XRD peaks after smoothing and non-linear curve fitting with the Gauss model. As a result, it was concluded that the average ZnO crystallite size was 35.36 nm, enough to be adsorbed on fabrics.

3.2. Coloration of Cotton and Polyester Fabrics in Violet and Yellow from Natural Dyes

In this research, two natural dyes, three types of UV protective treatment (including untreated samples), and four metallic mordants were applied to the 100% cotton and polyester weft fabrics. Table 1 and 2 indicate the color variation of Gromwell roots (GWR_V) and Cape Jasmine seeds (CJS_Y) dyed fabrics with various UV light absorbers and mordants. The Al-mordanted fabrics without any other treatments and post-mordants were categorized into 11C, 21C, 31C, 41C, 51C, and 61C of cotton weft samples and 12P, 22P, 32P, 42P, 52P, and 62P of polyester weft ones in both violet (Table 1) and yellow (Table 2) colors. The UV light-exposed fabrics were coded "sample name_0" to identify them before and after UV light testing.

In Table 1, it was evident that the color change occurred in the fabrics treated with ZnO/polyphenols. Compared with the pristine samples, the ZnO/polyphenol treated sample (31C to 37C) changed to yellowish and blighter with affected by phenolic gallnuts. The lightness values of the untreated samples (11C, 12P) were similar or slightly increased in those of the ZnO treated samples (21C, 22P). In terms of the impacts of post-mordants, the sample 37C, and 37P were distinctly darker and blackish because of iron sulfate mordanting. It was also seen that the UV light exposure caused distinguishable color changes between the unexposed violet dyed fabrics and the exposed ones to UV light due to fadedness. In contrast, the ZnO/gallnut treated samples did not exhibit considerable differences in fadedness.

Table 1. Categorization of Gromwell-roots dyed fabrics with various mordanting and UV protective treatments.

Dyes	Gromwell roots (Violet-dyes) [51] 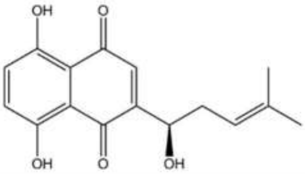 						
Fabrics	Cotton-weft twill			Polyester-weft twill			
Metallic mordants	UV photo absorber						UV light exposure
	Pristine	ZnO	ZnO/phenol	Pristine	ZnO	ZnO/phenol	
$KAl(SO_4)_2$	11C 	21C 	31C 	12P 	22P 	32P 	Before
	11C_0 	21C_0 	31C_0 	12P_0 	22P_0 	32P_0 	After
$Cu(OAc)_2$	15C 	25C 	35C 	15P 	25P 	35P 	Before
	15C_0 	25C_0 	35C_0 	15P_0 	25P_0 	35P_0 	After
$SnCl_2$	16C 	26C 	36C 	16P 	26P 	36P 	Before
	16C_0 	26C_0 	36C_0 	16P_0 	26P_0 	36P_0 	After
$FeSO_4$	17C 	27C 	37C 	17P 	27P 	37P 	Before

17C_0	27C_0	37C_0	17P_0	27P_0	37P_0	
						After

Table 2 illustrates the color variation of Cape Jasmine seeds (CJS-Y) dyed fabrics. Compared to the violet-dyed ones, the yellow-dyed fabrics did not represent severe color differences between the unexposed samples (41C to 67P) and the UV-light-exposed ones (41C_0 to 67P_0), in contrast with the GWR-Violet-dyed fabrics. The similarity of the yellow-dyed fabrics before and after UV light exposure was higher than the violet-dyed ones. To take a closer look, first, the Cu-mordanted samples revealed lower lightness than those of the pristine ones, whereas the Sn-mordanted samples became more chromatic. However, the UV-exposed samples with Sn-mordanting were clearly faded with much higher lightness than the unexposed ones. In addition, the hue of the ZnO/polyphenol-treated samples turned reddish. Last but not least, Fe-mordanting imparted the lowest lightness and the highest color strength to the ZnO/polyphenol-treated samples, followed by the ZnO-treated ones, then the untreated ones, in the order that stood out as 47C/47P > 57C/57P > 67C/67P. This effect of iron sulfate on yellow-dyed samples, conversely, differed from that on violet-dyed ones.

Table 2. Categorization of Cape Jasmine seeds dyed fabrics with various mordanting and UV protective treatments.

	Cape Jasmine seeds (Yellow-dyes) [26]						
Dyes	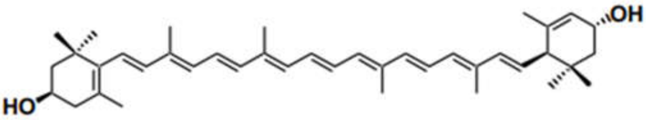						
Fabrics	Cotton-weft satin			Polyester-weft satin			
Metallic mordants	UV photo absorbers						UV light exposure
	Pristine	ZnO	ZnO/phenol	Pristine	ZnO	ZnO/phenol	
$KAl(SO_4)_2$	41C	51C	61C	42P	52P	62P	
							Before
	41C_0	51C_0	61C_0	42P_0	52P_0	62P_0	
							After
$Cu(OAc)_2$	45C	55C	65C	45P	55P	65P	
							Before
	45C_0	55C_0	65C_0	45P_0	55P_0	65P_0	
							After

3.3. Chromaticity of UV Absorbers and Metallic Mordants

Figure 4(a) and (b) illustrate the effects of metallic mordants on the chromatic variation of the fabrics dyed with shikonin or xanthophyll and treated without or with ZnO, ZnO/polyphenol. In general, the color of dyed cotton varied in a wider range than that of dyed polyester in this study. The distribution range of cotton samples was slightly broader in the v' axis than that of polyester samples, as confirmed in Table 1 and Table 2. In Figure 4(a), it was found that Sn-mordanting made the dyed fabrics brighter and blighter (higher lightness). The highest value of v′ coordinate was in 46C (0.5124) after Sn-mordanting in yellow hue, then 41C (0.5122) after Al-mordanting, and 45C (0.5107) after Cu-mordanting. The lowest v′ coordinate of 0.433 was located in sample 11C with the highest saturation. On the other hand, the chromaticity of yellow-dyed fabrics draws upward in the u' and v′ coordinates. In Figure 4 (b), the u′ coordinates of pre- and Sn-mordanted samples without UV treatments were greater than those with ZnO and ZnO/polyphenol treatments, in the following order: 41C/42P/46C >51C/52P/56C >61C/62P/66C. Interestingly, the distributed range of the ZnO/polyphenol-treated samples was narrow, not showing any greater dissimilarity than the treated cotton. It was also noteworthy that Fe-mordanting enabled the chromatic variation of yellow-dyed cotton and polyester to locate near the midpoint of (u′, v′ = 0.213, 0.480) coordinates of violet-dyed samples.

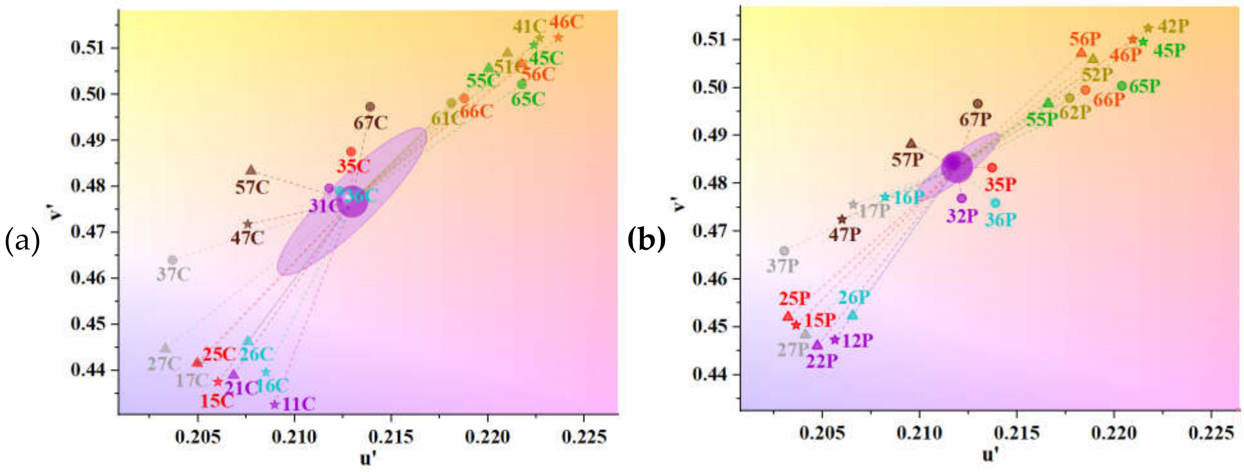

Figure 4. CIE diagrams of **(a)** cotton and **(b)** polyester fabrics dyed with shikonin and xanthophyll.

Using the chromaticity previously examined, Figure 5 demonstrates the effects of UV protective treatments on light absorbance from the reflectance spectra of the pristine samples and the treated ones. The Gromwell root colorants were shown to be most absorbed in the wavelength range of red to blue peaks at roughly 520, 560, and 600 nm in Figure 5(a). However, the ZnO/polyphenol-treated samples (31C, 32P) did not exhibit any clear peaks, implying a loss of red and blue hue. In Figure 5(b), the peak of yellow-dyed samples appeared at approximately 450 nm, which was slightly shifted towards 420–430 nm, where yellow color is usually absorbed. This phenomenon can be attributed to the bathochromic effect, as mentioned in other studies [23,41]. The lowest reflectance with the highest absorbance was seen in the yellow-dyed samples of 41C and 42P samples without the UV protective treatments in this study.

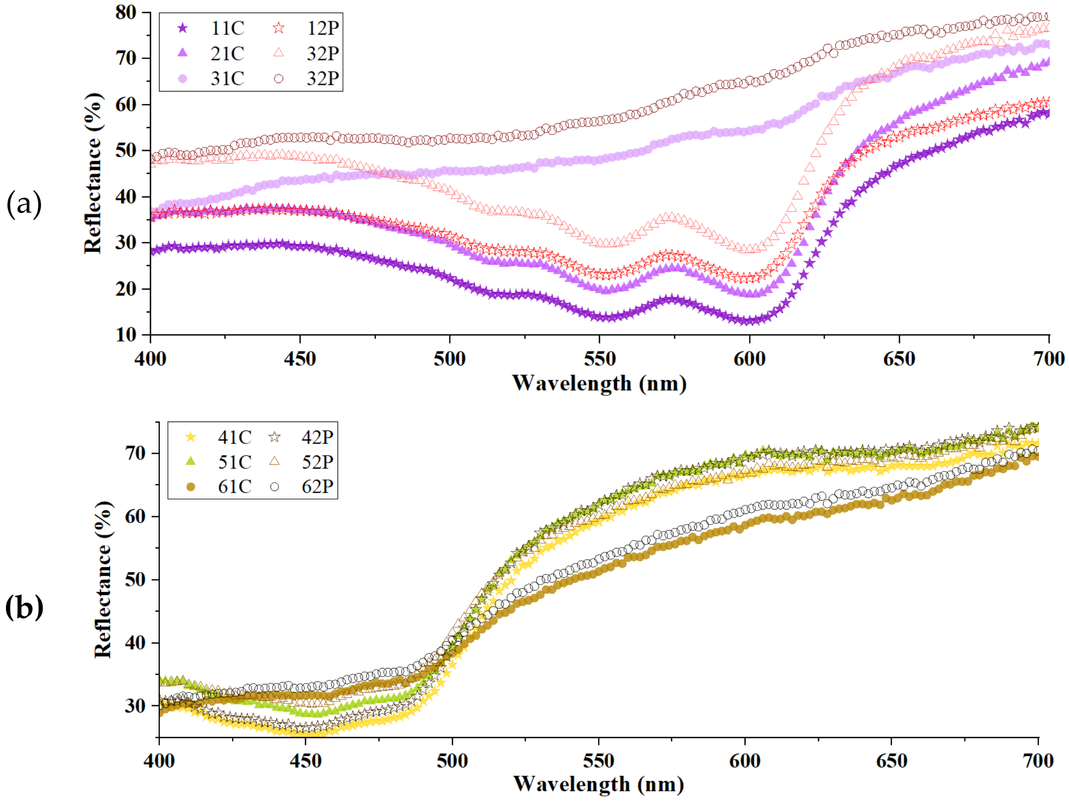

Figure 5. Reflective spectra of the cotton, polyester fabrics dyed with **(a)** shikonin and **(b)** xanthophyll with/without UV protective treatment.

In contrast to the aforementioned reflective curves, Figure 6 illustrates the CIELAB colorimetric parameters K/S and b* to compare the chromaticity of two chromophores, shikonin and xanthophyll. Overall, dramatic changes in colorimetric parameters were more prominent in the dyed cotton than the dyed polyester. In Figure 6(a), the highest K/S was found in sample 11C, representing the strongest violet color in a combination of red and blue hues. This is attributed to the aromatic ring (C=C) of phenyl groups in shikonin, which presumably contributed to the dye deposition on the cotton surface. The K/S values of 2.908 (11C) went downward to 1.749 (21C), followed by 0.716 (31C). This severe color change after UV treatment can be attributed to the absence of carbon-carbon double bonds in cotton, which made the chromophores permanently attached to the cotton [42]. The K/S values represent the color depth, or concentration after dyeing, which were related to the molar absorption coefficient from Beer-Lamber law and the auxochrome groups [23].

Compared with the violet-dyed fabrics, the yellow-dyed samples showed a gradual descent in K/S. Sample 41C displayed the greatest K/S value in the most intense yellow. The order of K/S values stands as: pristine samples >ZnO-treated samples >ZnO/polyphenol-treated samples, as agreed with the K/S order of violet-dyed samples. Therefore, it can be inferred that the insertion of ZnO and polyphenol decreased the color depth (K/S); however, the extent of the change in color strength (K/S) depended on the different components of natural dyes: naphthoquinone or β-carotenoid.

In Figure 6(b), the UV treatments led to yellowing in the shikonin-dyed samples; however, the xanthophyll-dyed samples decreased yellowness after UV treatment. The rise in b* from (-)15.705 to 7.722 was seen in violet-dyed fabrics, but not in yellow-dyed fabrics (mean 28.838). This can be due to the fact that cellulosic fibers accelerate yellowing because of the basic reaction of lignin and lignin peroxidase in alkali conditions, such as in DMSO for the ZnO treatment. Besides, UV protective treatments did not increase the lightness in yellow-dyed fabrics but in violet-dyed ones. This fact indicates the possibility that xanthophyll dyeing did not cause fadedness more than shikonin dyeing, yet it still needs further evidence.

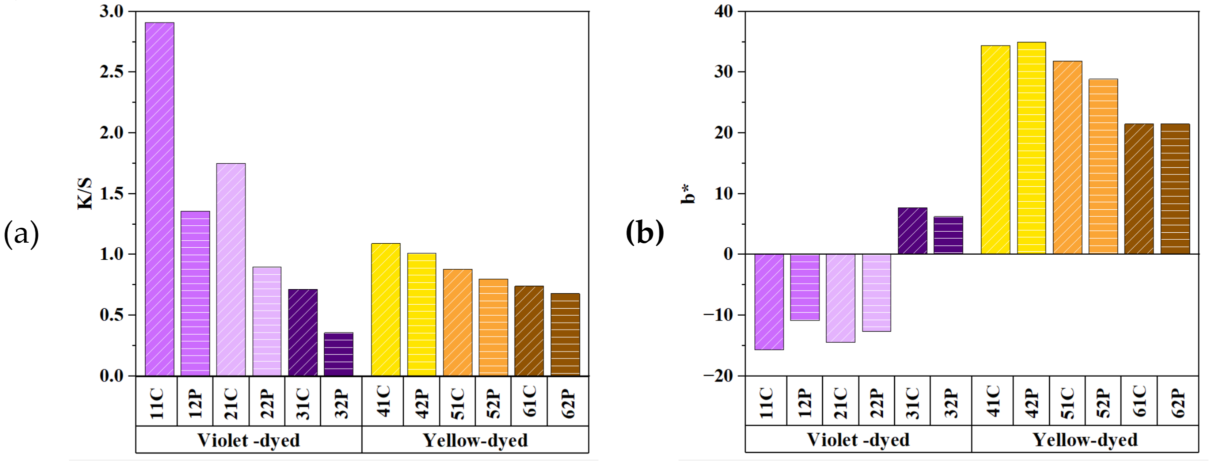

Figure 6. Colorimetric parameters of **(a)** K/S and **(b)** b* values of natural dyed cotton and polyester.

3.4. Comparison of Colorimetric Parameters with ZnO/Polyphenol Treatment after UV Exposure

To find the impacts of UV light exposure on the chromaticity, Figure 7 demonstrates the colorimetric K/S and b* parameters of the UV-treated fabrics without post-mordanted. Of the utmost importance, it was proven that the yellow dyeing with xanthophyll did not significantly discolor the fabrics even after UV exposure, compared with the violet dyeing. It was deduced that xanthophyll chromophores of carotenoids could prevent photooxidation more than shikonin chromophores of naphthoquinones because non-photochemical xanthophyll allowed fluorescence quenching to detoxicate reactive oxygen and dissipate excessive photon energy [43].

In Figure 7(a), the violet-dyed cotton samples without UV treatment revealed the most significant change in K/S. After being exposed to UV light, the highest K/S of sample 11C (2.908) drastically decreased to that of the untreated sample (0.695), indicating the untreated sample was the most powerfully faded. After exposure to UV light, the violet-dyed samples became less reddish and more yellowish, as pointed out in Figure 7(b). The UV-exposed samples in violet showed considerable increases in values b*, showing the highest rise of the samples (11C and 11C_0) from (-)15.71 to (+)11.54. In contrast, the yellow-dyed samples did not change considerably because the yellow hues did not turn bluish greatly with a small decrease in b* values. The b* values of UV-exposed samples (61C, 62P) were almost identical to the unexposed ones. It can be inferred that the carotenoid chromophores did not fade fabrics much due to the rapid equilibrium of isomerization and the excitation and oxidation of free radicals at low critical UV irradiation, despite other factors to consider [44,45].

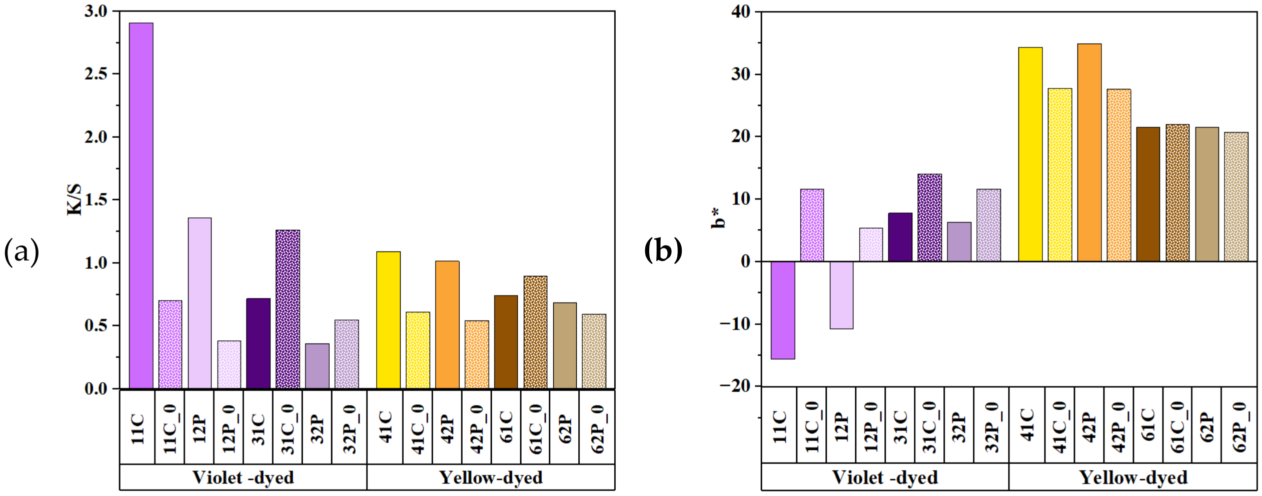

Figure 7. Comparison of **(a)** K/S and **(b)** b* values of the dyed fabrics without/with ZnO/polyphenol treatment between unexposed and exposed to UV light.

With the impacts of two natural dyes on the chromaticity above, Table 3 expresses the color differences (ΔE) of the dyed fabrics between unexposed and UV-exposed fabrics. In this study, the ΔE_{ab} was given from the UV-vis reflectance spectra using CIE1976 color space L a*b* coordinates, which were converted into L C*h* parameters to obtain the ΔE^*_{00} from the CIE2000 formula with weighing factors. These values were mathematically modified for the ΔE^*_{cmc} of the color tolerance CMC system with quasimetric parameters. This was because theoretically calculated chromatic values are inconsistent with human perception; hence, it is necessary to minimize the inconsistence of ΔE via various formulae, as suggested in several papers [31,32,46].

First, the color of violet-dyed samples changed much more substantially (mean ΔE: 20.42) than the yellow-dyed ones (mean ΔE: 5.57) after UV exposure, as already found in Figure 7. The biggest color difference was seen in the violet-dyed cotton untreated sample before and after UV light exposure, and the value of ΔE ranged from 37.03 (CIE1976), followed by 27.51 (CMC l:c=2:1), and 25.00 (CIEDE2000). The violet-dyed polyester samples generally discolored lower (mean ΔE:17.78) than the cotton ones (mean ΔE:23.07) under the same conditions.

Second, the ΔE narrowed down in the following order: the untreated samples >the ZnO-treated samples> the ZnO/polyphenol-treated samples. This tendency was the same as the ΔE_{cmc} order of the violet cotton, the violet polyester, and the yellow polyester. The negligible exception was found in the yellow cotton between the untreated samples (3.35) and the ZnO-treated ones (3.63). The least color difference (ΔE of 1.60) was seen in the ZnO/polyphenol-treated polyester (62P) in yellow dyeing. The average ΔE of all three models stood out in the order of the pristine violet (29.85)>the ZnO treated violet (26.75)>the ZnO/polyphenol treated violet (12.62)>the pristine yellow (9.62)>the ZnO treated yellow (5.50)>the ZnO/polyphenol treated yellow (3.23) dyed samples.

Third, the unexposed samples with the ZnO/polyphenol treatment did not differ from the UV-exposed ones. In Table 3, both ZnO/polyphenol-treated cotton and polyester in violet/yellow dyeing samples had a very narrow range of color differences (ΔE_{ab}: 6.60 and 6.22 in violet-dyeing, 2.60 and 1.60 in yellow-dyeing). The smallest ΔE was found in the ZnO/polyphenol-treated polyester (62P and 62P_0), the order of which stands as CIEDE2000 ΔE_{00} (2.44)> CIE1976 ΔE_{ab} (1.60)> CMC ΔE_{cmc} (1.06). Noteworthy, the color difference ΔE_{00} in CIEDE2000 was distributed with an even deviation. In conclusion, the ZnO/phenol treatments not only lower the K/S and chroma before exposure to UV light but also discolor at least both colored cotton and polyester fabrics even after UV exposure.

Table 3. Color difference of the violet, yellow dyed fabrics before and after exposure to UV light.

Sample	CIE1976 ΔE_{ab}	CMC ΔE_{cmc} (2:1)	CIEDE2000 ΔE_{00}	Mean ΔE±Std.
11C, 11C_0	37.03	27.51	25.00	29.85±6.35
21C, 21C_0	32.64	26.15	21.46	26.75±5.61

31C, 31C_0	6.60	8.70	22.57	12.62±8.68
12P, 12P_0	24.82	18.65	21.59	21.69±3.09
22P, 22P_0	22.26	18.26	21.61	20.71±2.15
32P, 32P_0	6.22	7.92	18.65	10.93±6.74
41C, 41C_0	7.49	3.35	18.01	9.62±7.56
51C, 51C_0	7.98	3.74	4.79	5.50±2.21
61C, 61C_0	2.60	1.13	5.95	3.23±2.47
42P, 42P_0	8.16	3.63	18.66	10.15±7.71
52P, 52P_0	4.46	2.22	2.90	3.19±1.15
62P, 62P_0	1.60	1.06	2.44	1.70±0.70

Table 4 shows the reflectance rates of the dyed fabrics in the UVB range (at 294 nm). Overall, the ZnO-treated samples reflected more UV light than the untreated ones, in contrast to the ZnO/polyphenol-treated samples, which had higher UV absorption. In Table 4, the reflectance rates increased to 13.60% (21C) from 11.14% (11C) and to 13.01% (22P) from 5.57% (12P) after the ZnO treatment. This increase in reflectance was consistent with the cotton and polyester in yellow by 2.13% (41C–51C). On the contrary, the reflectance rates sharply decreased from 11.14% to 3.84% in the violet-dyed cotton (11C–31C) after the ZnO/polyphenol treatment. This can be attributed to the hydroxyl groups of polyphenolic tannin, which can cross-link other molecules with their (-OH) bonds to improve dye affinity [33]. When the tannin from gallnut reacted with the shikonin chromophores, the double bond (C=C) aromatic rings from a phenolic compound could impart π-electron bonds to its carboxylic group, resulting in the improvement of UV absorption [47]. These findings can imply the effectiveness of the ZnO/phenol treatments on UV protection, despite their low color strength and chroma.

Table 4. Reflectance rates of the dyed cotton and polyester samples in UV-B (at 294 nm).

Violet-Dyed Sample	Reflectance (%)	Yellow-Dyed Sample	Reflectance (%)
11C	11.14	41C	8.81
21C	13.60	51C	10.94
31C	3.84	61C	3.70
12P	5.57	42P	7.43
22P	13.01	52P	7.57
32P	5.28	62P	3.69

3.5. Effects of Copper Acetate Mordants on UV Protection and Chromaticity

To take a closer examination of the UV photo absorber, Figure 8 illustrates how the ZnO/polyphenol affected the dyed samples with Cu-mordanted. In Figure 8 (a-d), all the reflectance spectra go downward from UVA (400 to 315 nm) to UVB (315 to 280 nm) ranges, with the excitonic absorption peak at 258 nm. The most prominent point was found in the Cu-mordanted samples with ZnO/polyphenol treatment before and after UV exposure. After Cu-mordanting, the reflectance rates of ZnO/polyphenol-treated samples were much lower than the untreated or the only ZnO-treated ones in UV-B. It was found that the combination of Cu-mordanting with ZnO/polyphenol treatments made the fabrics less reflective, i.e., more absorbent than the unexposed samples in UV-A. The hydroxyl groups from tannin provided good affinity with other molecules, resulting from the formation of hydrogen bonds [48]. In addition, the polyphenol could absorb UV rays from 300 to 360 nm, convert UV rays into heat, and finally delay photodegradation.

In addition, Cu-mordanting contributed to narrowing the gap between unexposed and UV-exposed samples. This phenomenon was predominant in the polyester fabrics dyed violet, as examined in Figure 8(b). In contrast to the high gap between the pristine polyester of samples 12P and 12P_0, the other Cu-mordanted samples after UV exposure showed almost identical reflectance to the unexposed samples. This can suggest the effectiveness of Cu-mordanting for UV protection.

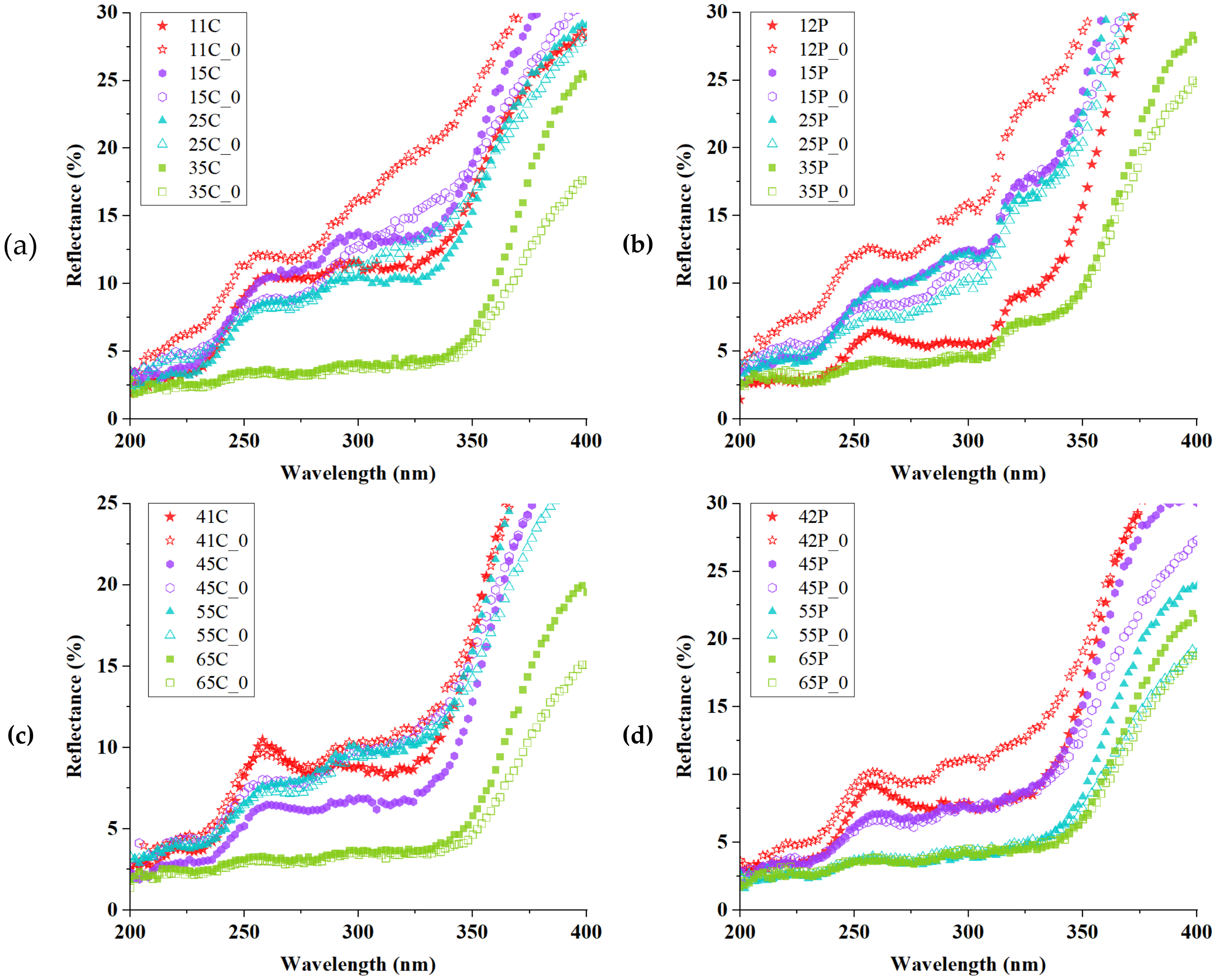

Figure 8. Reflectance curves of the violet-dyed **(a)** cotton, **(b)** polyester, and the yellow-dyed **(c)** cotton, and **(d)** polyester without/with Cu-mordanted before/after UV light exposure in the UVA and UVB ranges.

In Figure 8(d), all Cu-mordanted polyester samples in yellow dyeing were less reflective and more absorptive than the unexposed ones without Cu-mordant. The Cu-mordants could prohibit the reoccurrence of electron deficiency due to the chemical reduction of oxide compounds by the transferred electron from the excited state by light absorption. During the photo-induced charge separation, the electron acceptor generates negative charges that could react with metal ions, thereby forming Cu-chelate ligands [13,14]. The Cu-phenolic-chelating networks can impart the improvement of color strength and the fixation of UV absorbers to the ZnO/tannin-treated, Cu-mordanted, and dyed fabrics. Besides, UV light shielding can benefit from dyeing in darker hues or increasing color depth (K/S). Hence, Cu-mordanting can contribute to not just coloration by deepening color shades but also UV protection.

In Figure 9(a), the copper acetate mordants contributed to the enhancement in coloration of the ZnO/polyphenol-treated samples. The ZnO/polyphenol-treated sample with Cu-mordanting still kept its chroma and hue angles even better after UV exposure, as illustrated in Figure 9(b). This improvement could be attributed to the coordinate linkage of Cu^{2+} ions and carbonyl groups from the oxidation of phenols that were attached to the fabric surface, consistent with the previous study [49]. Consequently, the ZnO/polyphenol-treated sample with Cu-mordanting could colorize higher and more saturated chroma, as shown in Figure 9(a). However, the other samples seemed slightly faded, with lower chroma and changes in hue. When absorbing UV light, the xanthophyll chromophores could transfer the excited electrons to acceptors, lose the electrons, and then generate positive holes and hydroxyl or hyper-oxidative groups, which damaged the chromophores, leading to photodegradation [50].

Figure 9(b) exhibits the hue change of Cu-mordanted fabrics after UV exposure. The most important change was seen in the violet-dyed samples. The hue angles of the unexposed samples (15C/15/25C/25P) indicated the color of bluish violet, ranging from 315° to 317°. After being exposed to UV light, the hue angle shifted to reddish purple at approximately 50° to 68°. There was no significant difference between cotton and polyester samples in hue values.

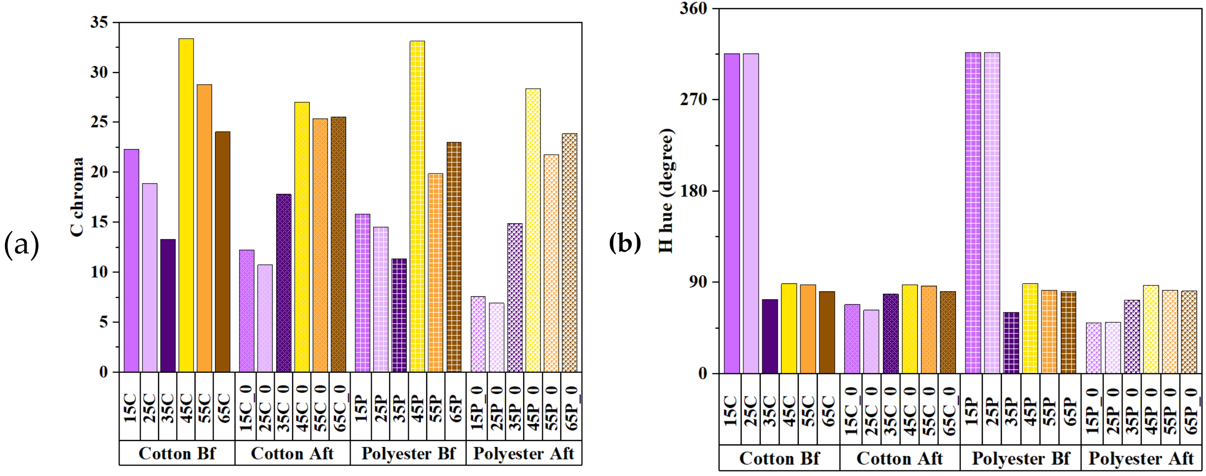

Figure 9. Comparison of **(a)** chroma and **(b)** hue angle values between Cu-mordanted cotton and polyester before and after UV exposure.

To find the effectiveness of ZnO/polyphenol treatments, Table 5 compares the ΔE between the unexposed and the UV-exposed samples, which were Cu-mordanted via three colorimetric formulae. The highest color differences (mean: 25.90±4.34) occurred of the untreated cotton fabrics in violet-dyeing. The second highest ΔE was shown in the untreated polyester fabrics in violet-dyeing (mean ΔE 16.03±2.72). In other words, the ZnO, ZnO, and polyphenol treatments helped the reduction in ΔE. Of importance, the color differences between yellow-dyed cotton and polyester were nearly zero, indicating that the UV exposure did not fade the 65C and 65P samples but rather turned them into improved color depth, as found in Figure 9(a, c). In the presence of ZnO/polyphenol, the unexposed and UV-exposed samples with xanthophyll-dyeing did not differ greatly from each other, showing a minute amount of ΔE 2.09±1.03 (cotton) and 0.69±0.30 (polyester), respectively. On the contrary, the ZnO/polyphenol treatments drastically decreased the ΔE from one sixth to one fourth in shikonin-dyed samples (mean: 4.42 to 4.43). In conclusion, it was articulated that the yellow-dyed fabrics that were Cu-post-mordanted and treated with ZnO/polyphenols were effective in increasing color similarity and decreasing color variation by UV light exposure.

Table 5. Comparisons in color differences (ΔE) between the unexposed and UV-exposed samples of Cu-mordanting with or without zinc oxide and polyphenol treatments.

Sample	CIE1976 ΔE_{ab}	CMC $\Delta E_{cmc\ (2:1)}$	CIEDE2000 ΔE_{00}	Mean ΔE±Std.
15C, 15C_0	30.27	25.83	21.59	25.90±4.34
15P, 15P_0	17.58	17.63	12.89	16.03 ± 2.72
35C, 35C_0	6.15	2.77	2.90	4.42±1.64
35P, 35P_0	4.55	2.26	3.13	4.43±1.24
45C, 45C_0	6.74	2.05	1.98	3.94±2.49
45P, 45P_0	4.45	1.07	1.12	2.58±1.70
65C, 65C_0	3.28	1.43	1.57	2.09±1.03
65P, 65P_0	1.00	0.65	0.41	0.69±0.30

doi:10.20944/preprints202405.1015.v1

4. Discussion

4.1. Strategies to Improve Chromaticity for UV Shielding

To improve UV protection and prevent discoloration, this study suggests three strategies: (1) natural dyeing with xanthophyll colorant; (2) ZnO/polyphenol treatment; and (3) Cu-post-mordanting. First, the xanthophyll chromophores in nature play a role in controlling the excessive amount of chlorophyll chromophores that were produced by much more intensive photo-energy. In other words, the xanthophyll is non-photochemical and normally screened by the chlorophyll, yet it appears in the absence of the chlorophyll. In this work, this natural phenomenon was imitated for the purpose of UV light shielding. Second, ZnO, as a photo-absorber, has either positive or negative effects on light fastness and photodegradation because of its redox-processability. Photodegradation efficiency may be accelerated by a high ZnO loading, but degradation can stabilize below a critical ZnO loading [19,50]. Polyphenolic tannic acid, as a bio-mordant, can fixate basic, cation, and reactive dyes onto fabric surfaces through the formation of covalent bonds with the dyes at pH levels that are controlled. Third, inorganic mordants, as auxochromes, can improve the diffusion, adsorption, and fixation of dye molecules, leading to the formation of a coordination complex. Metallic salts such as sodium carbonate, sodium sulfate, aluminum potassium sulfate, copper sulfate, and iron sulfate are unable to colorize themselves due to their non-photoabsorbency, but they can help the chromophores deepen the color shade variation of fabrics. Hydrophobic fabrics, such as polyester, whose high crystallinity makes it difficult to dye, require processing at high temperatures or under high pressure. The hydrophilic fabric, cotton, is susceptible to photo-oxidation; therefore, it is necessary for cellulose to transform photo-oxidative double bonds into photo-labile single bonds using hydrogen peroxides or oxidants for the prevention of photodegradation or the improvement of light fastness.

4.2. Limitation

There are some limitations to this research. The traditional procedures were used to process natural dyeing and mordanting. i.e., the dyeing parameters were already set, such as the concentration of dyes (the ratio of o.w.f.), the types of extract solvent, or the dyeing temperature. Second, the ZnO treatment was implemented after pre-mordanting and dyeing to prepare control samples for being pristine. It was known about the toxicity of ZnO when exposed to UV radiation for preventing sunscreen abuse. In addition, the excessive amount of ZnO use could be detrimental to cell longevity, hydrogen peroxide production, and the ecosystem's photosynthesis of phytoplankton [17]. However, further experiments concerning cytotoxicity were not conducted in this study. Third, the material selection was limited by the exclusion of toxic, carcinogenic mordants such as chromium or azoic dyes. There have been continuous concerns about waste dyeing water for marine ecosystems in the textile industry; therefore, this study aimed at the minimum discharge of dyeing wastes following traditional preparation for dyeing and mordanting. After experiments, the residue waste was collected as fertilizer.

5. Conclusions

In this work, the UV protective fabrics were prepared through natural dyeing with shikonin and xanthophyll colorants, ZnO/polyphenol treatment, and Cu-post-mordanting. The chromaticity of violet or yellow dyed fabrics was analyzed via UV-vis spectroscope with CIE colorimetric parameters of K/S, lightness, chroma, hue, a*, b*, and ΔE. As the results, the shikonin, in the combination with polyphenol caused the dyed cotton or polyester to vary extensively in chromaticity from violet to purple and brown to beige, with the highest K/S and the widespread variation. The violet dyeing led to the increase in the ΔE, and b* values, yet a decrease in the K/S, a*, chroma and hue angle. In contrast, the non-photochemical chromophores of xanthophyll contributed to the relatively coherent hue, chroma, and lightness in yellow compared with the violet dye fabrics. The ZnO treatment increased the reflectance rate in UVA-UVB ranges in UV-vis spectra, whereas the ZnO/polyphenol treatment could contribute to UV absorption, owing to tannin from gallnut. The Cu-mordants helped enhance the fixation of colorants, consequently minimizing the ΔE between non-exposed and UV-exposed samples. In this study, it was concluded that the combination of xanthophyll colorant, ZnO/polyphenol absorber, and Cu mordant was an effective strategy to shield UV light and protect skin.

Informed Consent Statement: Not applicable
Conflicts of Interest: None.

References

1. Ghazi, S. Do the polyphenolic compounds from natural products can protect the skin from ultraviolet rays?. *Results Chem*, **2022**. *4*, 100428. https://doi.org/10.1016/j.rechem.2022.100428
2. Kouassi, M. C.; Grisel, M.; Gore, E. Multifunctional active ingredient-based delivery systems for skincare formulations: A review. *Colloids and Surfaces B: Biointerfaces*, **2022**, 112676. https://doi.org/10.1016/j.colsurfb.2022.112676
3. Qin, J.; Guo, N.; Yang, J; Chen, Y. Recent Advances of Metal–Polyphenol Coordination Polymers for Biomedical Applications. *Biosensors*, **2023**, *13*(8), 776. https://doi.org/10.3390/bios13080776
4. Salvo, D.E; Gangemi, S; Genovese, C.; Cicero, N.; Casciaro, MPolyphenols from Mediterranean Plants: Biological Activities for Skin Photoprotection in Atopic Dermatitis, Psoriasis, and Chronic Urticaria. *Plants*, **2023**, *12*(20), 3579. https://doi.org/10.3390/plants12203579
5. Du, H.; Yue, M.; Huang, X.; Duan, G.; Yang, Z.; Huang, W.; Yin, X. Preparation, application and enhancement dyeing properties of ZnO nanoparticles in silk fabrics dyed with natural dyes. *Nanomater.* **2022**, *12*(22), 3953; *https://doi.org/10.3390/nano12223953*
6. Guan, W.; Zhang, L.; Wang, C.; Wang, Y. Theoretical and experimental investigations of the thermoelectric properties of Al-, Bi-and Sn-doped ZnO. *Mater. Sci. Semicond. Process.* **2017**, *66*, 247–252. https://doi.org/10.1016/j.mssp.2017.03.027
7. Jacob, J.; Rehman, U.; Mahmood, K.; Ali, A.; Mehboob, K.; Ashfaq, A.; Ashraf, F. Improved thermoelectric performance of Al and Sn doped ZnO nano particles by the engineering of secondary phases. *Ceram. Int*, **2020**, *46*(10), 15013-15017. https://doi.org/10.1016/j.ceramint.2020.03.031
8. Otaviano, B. T. H.; Sannomiya, M.; de Lima, F. S.; Tangerina, M. M. P.; Tamayose, C. I.; Ferreira, M. J. P.; da Costa, S. M. Pomegranate peel extract and zinc oxide as a source of natural dye and functional material for textile fibers aiming for photoprotective properties. *Mater. Chem. Phys*, **2023**, *293*, 126766. https://doi.org/10.1016/j.matchemphys.2022.126766
9. Vittal, R.; Ho, K. C. Zinc oxide based dye-sensitized solar cells: A review. *Renew. Sustain. Energy Rev.* **2017**, *70*, 920–935. https://doi.org/10.1016/j.rser.2016.11.273
10. Belay A.; Mekuria M,; Adam G. Incorporation of zinc oxide nanoparticles in cotton textiles for ultraviolet light protection and antibacterial activities. *Nanomater. Nanotechnolo.* **2020**, *10*. https://doi.org/10.1177/1847980420970052 https://doi.org/10.1177/184798042097005
11. Rise, M. S.; Ranjbar, A. H.; Noori, H.; Saheb, V. Synthesis and characterization of ZnO nanorods-Zn_2SiO_4 nanoparticles-PMMA nanocomposites for UV-C protection. *Opt. Mater.* **2022**, *123*, 111922. https://doi.org/10.1016/j.optmat.2021.111922
12. Baranei, M.; Taheri, R. A.; Tirgar, M.; Saeidi, A.; Oroojalian, F.; Uzun, L.; Goodarzi, V. Anticancer effect of green tea extract (GTE)-Loaded pH-responsive niosome Coated with PEG against different cell lines. *Mater. Today Commun.* **2021**, *26*, 101751. https://doi.org/10.1016/j.mtcomm.2020.101751
13. Brza, M.A.; Shujahadeen B.; Aziz, H.; Anuar, Fathilah Ali, Elham M.A.; Dannoun, Salah R.; Saeed, Sewara J.; Mohammed, Rebar T. Abdulwahid. Green coordination chemistry as a novel approach to fabricate polymer:Cd(II)-complex composites: Structural and optical properties. *Opt. Mater.* **2021**, *116*, 111062. https://doi.org/10.1016/j.optmat.2021.111062
14. Feng, Y.; Li, P.; Wei, J. Engineering functional mesoporous materials from plant polyphenol based coordination polymers. *Coord. Chem. Rev.* 2022, *468*, 214649. https://doi.org/10.1016/j.ccr.2022.214649
15. Fernandes, S. C.; Alonso-Varona, A.; Palomares, T.; Zubillaga, V.; Labidi, J.; Bulone, V. Exploiting mycosporines as natural molecular sunscreens for the fabrication of UV-absorbing green materials. *ACS Appl. Mater. Interfaces.* **2015**, *7*(30), 16558-16564.
16. Luo, J.; Liu, Y.; Yang, S.; Flourat, A. L.; Allais, F.; Han, K.Ultrafast barrierless photoisomerization and strong ultraviolet absorption of photoproducts in plant sunscreens. *J. Phys. Chem. Lett.* **2017**, *8(5),* 1025-1030. https://doi.org/10.1021/acs.jpclett.7b00083
17. Sen, S.; Mallick, N. Mycosporine-like amino acids: Algal metabolites shaping the safety and sustainability profiles of commercial sunscreens. *Algal Res.* **2021**, *58*, 102425. https://doi.org/10.1016/j.algal.2021.102425
18. He, Y.; Li, N.; Xiang, Z.; Rong, Y.; Zhu, L.; Huang, X. Natural polyphenol as radical inhibitors used for DLP-based 3D printing of photosensitive gels. *Mater. Today Commun.* **2022**, *33*, 104698. https://doi.org/10.1016/j.mtcomm.2022.104698

19. Groeneveld, I.; Kanelli, M.; Ariese, F.; van Bommel, M. R. Parameters that affect the photodegradation of dyes and pigments in solution and on substrate–An overview. *Dyes Pigm.* **2023**, *210*, 110999. https://doi.org/10.1016/j.dyepig.2022.110999
20. Rader Bowers LM; Schmidtke Sobeck SJ. Impact of medium and ambient environment on the photodegradation of carmine in solution and paints. *Dyes Pigm.* **2016**, *127*:18–24. https://doi.org/10.1016/J.DYEPIG.2015.12.012.
21. Michelin, C.; Hoffmann, N. Photosensitization and photocatalysis—Perspectives in organic synthesis. *ACS Catal.* **2018**, *8*(12), 12046-12055. https://doi.org/10.1021/acscatal.8b03050
22. Abiola, T. T.; Whittock, A. L.; Stavros, V. G. Unravelling the photoprotective mechanisms of nature-inspired ultraviolet filters using ultrafast spectroscopy. *Mol.* **2020**, *25*(17), 3945; https://doi.org/10.3390/molecules25173945
23. Deniz, N. G.; Iscan, A.; Sayil, C.; Avinc, O.; Kalayci, E. Naphthoquinone disperse dyes and their dyeing application to polyethylene terephthalate fabrics. *J. Text. Inst.* **2023**, 1-15. https://doi.org/10.1080/00405000.2023.2271667
24. Dulo, B.; Phan, K.; Githaiga, J. Natural Quinone Dyes: A Review on Structure, Extraction Techniques, Analysis and Application Potential. *Waste Biomass Valor*, **2021**, *12*, 6339–6374 https://doi.org/10.1007/s12649-021-01443-9
25. La, E. H.; Giusti, M. M. Ultraviolet–Visible Excitation of cis-and trans-pC oumaric Acylated Delphinidins and Their Resulting Photochromic Characteristics. *ACS Food Sci. Tech.* **2022**, *2*(5), 878-887. https://doi.org/10.1021/acsfoodscitech.2c00028
26. Maoka, T. Carotenoids as natural functional pigments. *J Nat Med.* **2020**, *74*, 1–16 https://doi.org/10.1007/s11418-019-01364-x
27. Rafiq, A.; Ikram, M.; Ali, S.; Niaz, F.; Khan, M.; Khan, Q.; Maqbool, M. Photocatalytic degradation of dyes using semiconductor photocatalysts to clean industrial water pollution. *Ind. Eng. Chem. Res.*, **2021**, *97*, 111–128. https://doi.org/10.1016/j.jiec.2021.02.017
28. Canopoli, L.; Coulon, F.; Wagland, S. T. Degradation of excavated polyethylene and polypropylene waste from landfill. *Sci. Total Environ. 2020*, *698*, 134125. https://doi.org/10.1016/j.scitotenv.2019.134125
29. Wang, X.; Sun, X.; Guan, X.; Wang, Y.; Chen, X.; Liu, X. Tannic interfacial linkage within ZnO-loaded fabrics for durable UV-blocking applications. *Appl. Surf. Sci.* **2021**, 568, 150960. https://doi.org/10.1016/j.apsusc.2021.150960
30. Ayesha, B.; Jabeen, U.; Naeem, A.; Kasi, P.; Malghani, M. N. K.; Khan, S. U.; Aamir, M. Synthesis of zinc stannate nanoparticles by sol-gel method for photocatalysis of commercial dyes. *Results Chem.* **2020**, *2*, 100023. https://doi.org/10.1016/j.rechem.2020.100023
31. Wang, X.; Jiang, Y.; Du, J.; Xu, C. Establishment of a color tolerance for yarn-dyed fabrics from different color-depth yarns. *Color Res. Appl.*, **2022**, *47*(1), 225-235. https://doi.org/10.1002/col.22711
32. He, R.; Xiao, K.; Pointer, M.; Melgosa, M.; Bressler, Y. Optimizing Parametric Factors in CIELAB and CIEDE2000 Color-Difference Formulas for 3D-Printed Spherical Objects. *Mater.* **2022**, *15*, 4055. https://doi.org/10.3390/ma15124055
33. Repon, M. R.; Dev, B.; Rahman, M. A.; Jurkonienė, S.; Haji, A.; Alim, M. A.; Kumpikaitė, E. Textile dyeing using natural mordants and dyes: a review. *Environ. Chem. Lett.* **2024**. https://doi.org/10.1007/s10311-024-01716-4
34. An, N.; Hu, J; Ding, Y; Sheng, P; Zhang, Z; Guo, X. Ionic liquid treated cellulose-based intelligent pH-responsive color indicator film, with excellent anti-ultraviolet function. *J. Polym. Res.* **2023**, *30*(9), 343. https://doi.org/10.1007/s10965-023-03716-4
35. Soosairaj, A; Pabba, D.P; Gunasekaran, A. et al. Synergetic impact of natural light harvesting materials to reduce the recombination rate and improve the device performance of dye sensitized solar cells. *J Mater Sci: Mater. Electron.* **2023**, *34*, 1748 https://doi.org/10.1007/s10854-023-11172-5
36. Sun, Q; Gong, T; Liu, M; Ren, S; Yang, H; Zeng, S; Xu, H. Shikonin, a naphthalene ingredient: Therapeutic actions, pharmacokinetics, toxicology, clinical trials and pharmaceutical researches. *Phytomedicine*, **2022**, *94*, 153805. https://doi.org/10.1016/j.phymed.2021.153805
37. Jeyaram, S. Spectral, third-order nonlinear optical and optical switching behavior of β-carotenoid extracted from phyllanthus niruri. *Ind. J. Phys.* **2022,** *96*(6), 1655-1661. https://doi.org/10.1007/s12648-021-02122-0
38. Lin, P; Chen, L; Huang, X; Xiao, F; Fu, L; Jing, D; Wu, Y. Structural characteristics of polysaccharide GP2a in Gardenia jasminoides and Its Immunomodulatory Effect on Macrophages. *Int. J. Mol. Sci.* **2022**, *23*(19), 11279. https://doi.org/10.3390/ijms231911279
39. Adedokun, O; Adedeji, O. L; Bello, I. T; Awodele, M. K; Awodugba, A. O. Fruit peels pigment extracts as a photosensitizer in ZnO-based Dye-Sensitized Solar Cells. *Chem. Phys.* **2021**, *3*, 100039. https://doi.org/10.1016/j.chphi.2021.100039
40. Lee, J; Kang, M. H; Lee, K. B; Lee, Y. Characterization of natural dyes and traditional Korean silk fabric by surface analytical techniques. *Mater.* **2013**, *6*(5), 2007-2025. https://doi.org/10.3390/ma6052007

41. Silva, P. M. D. S; Fiaschitello, T. R; Queiroz, R. S. D; Freeman, H. S; Costa, S. A. D; Leo, P; Costa, S. M. D. Natural dye from Croton urucurana Baill. bark: extraction, physicochemical characterization, textile dyeing and color fastness properties. *Dyes Pigm.* **2020**, *173*, 01–14. https://doi.org/10.1016/j.dyepig.2019.107953
42. Liman, M. L. R; Islam, M. T; Repon, M. R; Hossain, M. M; Sarker, P. Comparative dyeing behavior and UV protective characteristics of cotton fabric treated with polyphenols enriched banana and watermelon biowaste. *Sustain. Chem. Pharm.* **2021**, *21*, 100417. https://doi.org/10.1016/j.scp.2021.100417
43. Badmus, U. O; Ač, A; Klem, K; Urban, O; Jansen, M. A. A meta-analysis of the effects of UV radiation on the plant carotenoid pool. *Plant Physiol Biochem.* **2022**, *183*, 36–45. https://doi.org/10.1016/j.plaphy.2022.05.001
44. La, E. H; Giusti, M. M. Ultraviolet–Visible Excitation of *cis-* and *trans-p*Coumaric Acylated Delphinidins and Their Resulting Photochromic Characteristics. *ACS Food Science & Technology*, 2022, *2*(5), 878-887.
45. Jiang, H; Hu, X; Khan, A; Yao, J; Tahir Hussain, M. Dyeing mechanism and photodegradation kinetics of gardenia yellow natural colorant. *Text. Res. J.* **2021**, *91*(7-8), 839-850. https://doi.org/10.1177/0040517520958483
46. Seymour, J. Color inconstancy in CIELAB: A red herring?. *Color Res. Appl. 2022*, *47*(4), 900-919
47. Wulansari, A. D; Hayati, D; Long, D. X; Choi, K; Hong, J. Hydroxycinnamic acid derivatives for UV-selective and visibly transparent dye-sensitized solar cells. *Sci. Rep.* **2023**, *13*(1), 3235. https://doi.org/10.1038/s41598-022-17236-6
48. Baldwin. A; and Booth. B. W. Biomedical applications of tannic acid. *J. Biomater. Appl.* **2022**, *36* (8), 1503-1523. https://doi.org/10.1177/08853282211058099
49. Amir, M; Ahmed, K; Hasany, S. F; Butt, R. A. Non-Covalent Bonding of Green Synthesized Copper Nanoparticles to enhance Physicochemical behavior of Sulfur-Dyed Cotton Fabric. *AATCC J. Res.* **2023**, *10*(5), 280-288. https://doi.org/10.1177/24723444231116174
50. Saeed K, Khan I, Gul T, Sadiq M. Efficient photodegradation of methyl violet dye using TiO_2/Pt and TiO_2/Pd photocatalysts. *Appl Water Sci* **2017**; *7*:3841–8. https://doi.org/10.1007/s13201-017-0535-3.
51. Guo, C; He, J; Song, X; Tan, L; Wang, M; Jiang, P; Peng, C. Pharmacological properties and derivatives of shikonin—A review in recent years. *Pharmacol. Res. Commun*, **2019**, *149*, 104463. https://doi.org/10.1016/j.phrs.2019.104463
52. Bruce Lindbloom. Available online: www.brucelindbloom.com (accessed on 19 February 2024).